*arthropoda*

MDPI

*Article*

# A New Species of *Proctolaelaps* (Acari: Mesostigmata: Ascoidea: Melicharidae) Associated with Ambrosia Beetles (Coleoptera: Curculionidae: Scolytinae: Xyleborini) in South Florida Avocados †

**Marielle M. Berto [1], Raphael de Campos Castilho [2], Aline D. Tassi [1], Avyla Regia de Albuquerque Barros [2] and Daniel Carrillo [1,*]**

[1] Tropical Research and Education Center, Department of Entomology and Nematology, University of Florida, Homestead, FL 33031, USA; mdemoraesberto@ufl.edu (M.M.B.); aline.tassi@ufl.edu (A.D.T.)
[2] Escola Superior de Agricultura Luiz de Queiroz (ESALQ), Universidade de São Paulo (USP), Piracicaba 13418-900, São Paulo, Brazil; raphael.castilho@usp.br (R.d.C.C.)
* Correspondence: dancar@ufl.edu
† urn:lsid:zoobank.org:pub:D11DA8AA-944A-429A-A2EB-B3F30905DEDB.

**Abstract**

A new species of *Proctolaelaps* (Acari: Mesostigmata: Melicharidae), *Proctolaelaps ambrosiae* sp. nov., is described from south Florida, USA, based on adult females found in phoretic association with ambrosia beetles infesting avocado (*Persea americana*) trees. Mites were removed from adults of *Xyleborinus saxesenii* and *Xyleborus affinis* (Coleoptera: Curculionidae: Scolytinae: Xyleborini) captured in flight and were also collected from beetle galleries in infested avocado wood. The new species is diagnosed based on a combination of morphological characters and molecular markers (nuclear 28S rRNA and ITS, and mitochondrial COI), supporting its distinctiveness from related taxa. This study represents the first formal description of a *Proctolaelaps* species documented in phoretic association with xyleborine ambrosia beetles and their galleries, contributing to the knowledge of melicharid diversity in woody microhabitats and providing baseline data for future ecological and applied studies of ambrosia beetle systems in avocado.

**Keywords:** mites; taxonomy; phoresy; molecular markers; ambrosia beetles

## 1. Introduction

The genus *Proctolaelaps* Berlese is the most taxonomically diverse and widespread group within the family Melicharidae (Mesostigmata: Ascoidea), with at least 154 species described to date [1–5]. Many species in this genus use arthropods for dispersal via phoresy, a commensalistic association that enables mites to exploit ephemeral microhabitats such as decaying wood, fungal bodies, flowers, or leaf litter [5–14].

Several *Proctolaelaps* species are known for their affinity for woody habitats and for phoretic associations with bark beetles (Coleoptera: Curculionidae: Scolytinae), eventually establishing long-term relationships with their hosts and inhabiting beetle breeding sites within constructed galleries [8,15–18]. Within the Scolytinae, ambrosia beetles represent a distinct ecological group characterized by fungus farming in the xylem of host trees [18]. Several ambrosia beetle species have become major global pests in natural and agricultural ecosystems due to their association with plant pathogens. This has led to extensive research on their behavior within tree hosts and gallery formation processes [19], flight activity and

Check for updates

Academic Editor: Anna Seniczak

Received: 23 December 2025
Revised: 11 February 2026
Accepted: 25 February 2026
Published: 28 February 2026

**Copyright:** © 2026 by the authors. Licensee MDPI, Basel, Switzerland. This article is an open access article distributed under the terms and conditions of the Creative Commons Attribution (CC BY) license.

distribution in cropping systems [20], and fungal symbiotic associations [21,22], particularly those involving plant pathogens [23,24]. In the United States, avocado (*Persea americana* Mill.; Lauraceae) production in Florida has been severely impacted by laurel wilt, a lethal fungal disease transmitted by ambrosia beetles of the tribe Xyleborini [21,23].

Most studies of ambrosia beetle symbiosis have focused on their fungal partners. However, other organisms involved in these systems, including nematodes [25,26] and phoretic mites, have received little attention [27–29], and their roles in this multipartite symbiosis remain largely unknown. Investigating phoretic associations involving ambrosia beetles is particularly important given the potential of melicharid mites as biological control agents of economically significant agricultural pests [13]. During a survey of mite fauna associated with ambrosia beetles on avocado trees in Florida, USA, an undescribed species of *Proctolaelaps* was discovered. To date, 37 species of this genus have been recorded from the USA, seven of which are associated with scolytine bark beetles [2]. Among these, *Proctolaelaps subcorticalis* Lindquist and *Proctolaelaps xyloteri* Samšiňák have been reported in the USA in association with the striped ambrosia beetle, *Trypodendron lineatum* (Olivier) (Scolytinae: Scolytini) [2,16,30], which is considered one of the major forest pests in the Holarctic region [31].

This study presents a detailed morphological description of a new *Proctolaelaps* species, supported by illustrations and molecular analysis, thereby expanding our understanding of ecological diversity within the family Melicharidae.

## 2. Materials and Methods

### *2.1. Mite Collection*

Modified Lindgren multiple funnel traps [32] were deployed in three avocado orchards in Miami-Dade County (25°30′44.24″ N, 80°31′10.03″ W; 25°32′17.72″ N, 80°29′10.77″ W; and 25°35′41.04″ N, 80°28′20.57″ W), Florida, USA, in March 2023 to capture adult ambrosia beetles in flight. The modification consisted of replacing the standard collection cup with a plastic bag (46 × 20 cm; height × diameter) containing wet paper towel sheets to collect beetles alive. Traps were baited with ultra-high release ethanol lures (Alpha Scents, Canby, OR, USA), deployed in the late afternoon, and retrieved early the following morning to encompass the crepuscular flight period of most ambrosia beetles inhabiting avocado groves [32,33].

In addition, ambrosia beetle-infested logs were collected from the avocado orchards and transported to the Tropical Fruit Entomology Lab (University of Florida—Tropical Research and Education Center), where they were split open using various wood-cutting tools (e.g., manual log splitters, chisels, and hammers) to expose galleries. Exposed galleries were examined under a stereomicroscope for the presence of ambrosia beetles and associated mites.

Mites attached to adult beetles in flight or found within their galleries were directly mounted in Hoyer's medium for identification using Differential Interference Contrast Microscopy (Zeiss Axio Imager M2). A subset of the field-collected individuals was used to establish a laboratory colony as described by Berto et al. [28].

### *2.2. Morphological Description*

Specimens belonging to Melicharidae were identified using the family-level taxonomic key developed by Lindquist et al. [34], while the genus *Proctolaelaps* was recognized based on diagnostic features outlined by Moraes et al. [1]. Comparisons with original descriptions and subsequent redescriptions available in the literature indicated that these specimens represent an undescribed species, which is formally described in this study.

All measurements of taxonomically important structures are provided in micrometers, with mean values followed by ranges in parentheses. Shield lengths were measured along the midline from the anterior to the posterior margins, and widths at their widest point unless otherwise noted. Leg lengths were measured from the base of the coxa to the apex of the tarsus, excluding the pretarsus.

Idiosomal setal terminology follows the systems proposed by Lindquist & Evans [35] and Lindquist [36], with additional guidance from Lindquist & Moraza [37]. Leg and palp chaetotaxy follows Evans [38,39]. The interpretation of pore-like structures is based on Athias-Henriot [40,41].

### *2.3. Molecular Characterization*

Genomic DNA was extracted from six adult females from the laboratory colony [28]. Extractions were performed using the DNeasy Blood & Tissue Kit (Qiagen, Hilden, Germany), following the manufacturer's protocol with minor modifications suitable for minute invertebrates such as mites [42]. After DNA extraction, mite specimens were carefully recovered from the spin columns and subsequently slide-mounted in Hoyer's medium for preservation. These vouchers are deposited at the Tropical Fruit Entomology Laboratory, University of Florida, Homestead, USA, and serve as taxonomic reference material.

Four molecular markers were selected for amplification to support species identification and phylogenetic analyses: 12S rRNA, cytochrome c oxidase subunit I (COI), 28S rRNA, and the internal transcribed spacer (ITS) region. Despite repeated optimization attempts, consistent amplification of 12S rRNA was unsuccessful, and this marker was therefore excluded from subsequent analyses. The remaining three markers were successfully amplified using established primer sets:

- 28S rRNA: primers 43F (5′-GCTGCGAGTGAACTGGAATCAAGCCT-3′) and 929R (5′-AGGTCACCATCTTTCGGGTC-3′) [43],
- ITS region: primers ITS-F (5′-AGAGGAAGTAAAAGTCGTAACAAG-3′) and ITS-R (5′-ATATGCTTAAATTCAGGGGG-3′) [44],
- COI mitochondrial DNA: universal primers LCO1490 (5′-GGTCAACAAATCATAAAGATATTGG-3′) and HCO2198 (5′-TAAACTTCAGGGTGACCAAAAAATCA-3′) [45].

PCR amplifications were performed in 25 µL reaction volumes using the DreamTaq™ Hot Start polymerase system (Thermo Fisher Scientific, Waltham, MA, USA), following the manufacturer's recommendations. Thermal cycling conditions were optimized for each genetic marker as specified in the corresponding references. Amplification success was initially assessed by electrophoresis on a 1.0% agarose gel stained with SYBR™ Safe DNA gel stain (Invitrogen, Waltham, MA, USA). Samples showing successful amplification were subsequently run on a 1.5% low-melting-point agarose gel and stained with SYBR™ Safe to facilitate DNA band excision. Well-defined DNA bands were excised using an x-trata™ gel extraction tool (Promega, Madison, WI, USA) and purified with the Wizard® SV Gel and PCR Clean-Up System (Promega), according to the manufacturer's protocol. Successfully amplified fragments corresponding to COI, 28S rRNA, and ITS regions were subjected to bidirectional Sanger sequencing by Eurofins Genomics (Louisville, KY, USA).

Forward and reverse chromatograms were assembled into consensus sequences and quality-checked using the Staden Package v1.6.0, with Pregap4 used for automated initial processing and Gap4 for contig assembly and inspection. No manual editing or base-calling corrections were applied to the raw sequence chromatograms.

The accuracy of COI sequence alignments was evaluated by translating the aligned nucleotide sequences into amino acids using the ExPASy Translate Tool (https://web.expasy.org/translate/; accessed on 15 October 2025) to verify the absence of internal stop codons or frameshifts. Putative protein-coding regions were further examined by identifying open

reading frames using ORFfinder (https://www.ncbi.nlm.nih.gov/orffinder/; accessed on 15 October 2025). To detect aberrant or atypical sequences, all sequences were additionally screened using SmartBLAST implemented at the National Center for Biotechnology Information (https://blast.ncbi.nlm.nih.gov/smartblast/smartBlast.cgi; accessed on 15 October 2025).

Consensus sequences were compared with available GenBank data using BLAST algorithms (http://blast.ncbi.nlm.nih.gov/Blast.cgi; accessed on 15 October 2025). To investigate the phylogenetic placement of the mite specimens, reference sequences for the 28S rRNA, ITS, and COI gene regions from a range of representative Mesostigmata taxa were retrieved from GenBank (see Table S1).

Multiple sequence alignments were performed using the ClustalW algorithm implemented in MEGA version 11 with default gap-opening and gap-extension penalties [46,47]. Alignments were manually inspected and refined to correct misalignments and optimize positional homology. Low-quality terminal positions with excessive missing data were trimmed prior to phylogenetic inference to ensure reliable positional homology. Missing data were treated as gaps in all analyses.

Evolutionary histories were inferred using maximum-likelihood methods implemented in MEGA version 11. The best-fit nucleotide substitution model for each marker was selected independently based on the Bayesian Information Criterion (BIC) [43,44]. The selected models were TN93+G (28S), T92+G (ITS), and T92+G (COI), with among-site rate heterogeneity modeled using a discrete gamma distribution. Nodal support was assessed using nonparametric bootstrap resampling with 1000 replicates. Branch lengths are expressed as the number of substitutions per site.

## 3. Results

### *3.1. Description*

***Proctolaelaps ambrosiae*** **Berto & Castilho sp. nov.**

*Diagnosis (female)*

Fixed cheliceral digit with the 5–6 min teeth immediately behind the apical tooth, followed by seven larger teeth. Palp tarsal claw 2-tined, with the bulbous base. Anterior margin of epistome with three aciculate extensions. Subcapitular setae acicular and smooth. Podonotal region of dorsal shield mostly smooth, except anterolaterally, striated. Dorsal shield with 43 pairs of dorsal shield setae, including five pairs of marginal setae (*R1–R5*) in the opisthonotal region. Seta *j4* about half the distance between its base and the base of *j5*. Presence of a finely denticulate line connecting the bases of setae *J5.* Unsclerotized idiosomal cuticle with 14 pairs of setae (*R6*, *UR1*, *UR3–UR5*, *Jv1–Jv5*, *Zv1–Zv3*, and *Zv5*). Presence of three pairs of metapodal platelets.

FEMALE (six specimens measured)

Gnathosoma. Fixed cheliceral digit 22 (20–25) long (from apex to dorsal lyrifissure), with the 5–6 min teeth immediately behind the apical tooth, followed by seven larger teeth (Figure 1); with dorsobasal pointed process barely discernible and a broad hyaline lobe; hyaline rim along the paraxial face of the cheliceral shaft above base of movable digit with tiny denticles; movable cheliceral digit 23 (20–24) long, with three relatively large teeth in addition to the apical tooth, with a robust ventral projection; antiaxial and dorsal lyrifissures as well as dorsal seta distinct. Number of setae on palp trochanter-tarsus: 2-5-6-14-15; setae aciculate and smooth, except femur *al* as well as genu *al2*, spatulate and smooth (Figure 2); palp tarsal claw 2-tined, with the bulbous base (Figure 3). Anterior margin of epistome with three aciculate extensions (Figure 4). Deutosternum with seven roughly transverse lines; the anterior-most smooth, while the others with 2–7 denticles, except the most basal, extending

beyond the margins of the deutosternum, with 16–19 denticles (Figure 5). Internal malae reaching the level of the tip of corniculi; outer margin denticulate and inner margin smooth. Corniculi horn-like, with a small projection near the base; 20 (17–23) long and 7 (7–8) wide at the widest level, well separated from each other. Seta *h3* longitudinally aligned with *h*1, and slightly posteriad and mediad *h2*. Measurements of setae: *h1* 27 (26–28), *h2* 16 (14–18), *h3* 29 (27–31), *pc* 19 (18–20); all acicular and smooth.

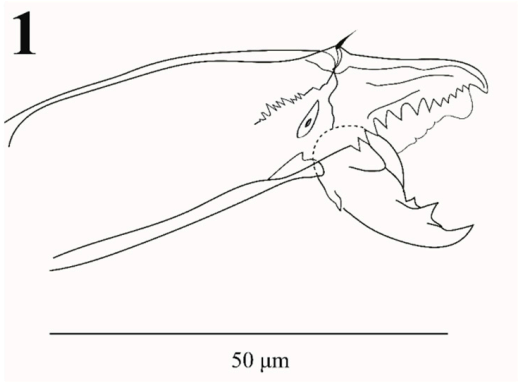


**Figure 1.** *Proctolaelaps ambrosiae* sp. nov., adult female. Lateral (antiaxial) view of chelicera.

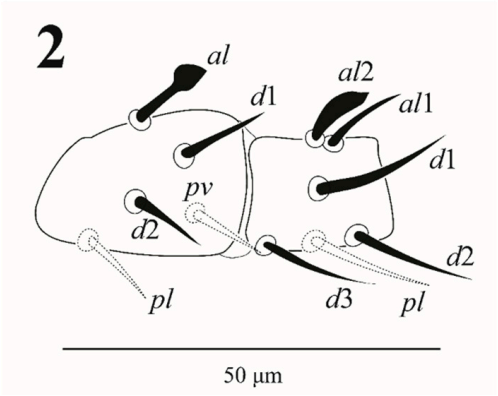


**Figure 2.** *Proctolaelaps ambrosiae* sp. nov., adult female. Palpal femur and genu.

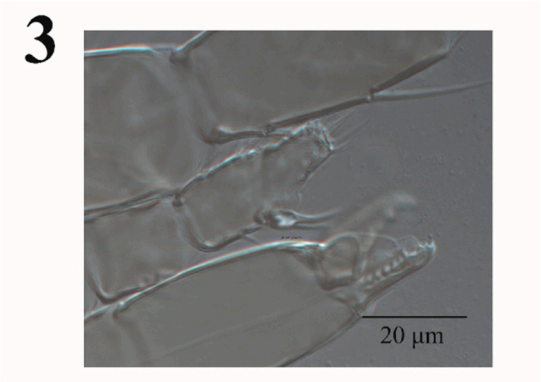


**Figure 3.** *Proctolaelaps ambrosiae* sp. nov., adult female. Palp tarsal claw (DIC micrograph).

Dorsal idiosoma (Figure 6). Dorsal shield 340 (321–353) long and 174 (160–185) wide. Podonotal region mostly smooth, except anterolaterally, striated; with 23 pairs of setae (*j1–j6*, *z1–z6*, *s1–s6*, and *r2–r6*), five pairs of distinguishable lyrifissures, and four pairs of distinguishable gland pores. Opisthonotal region striated, with a delineated strip along the lateral margin, bearing several *r-R* setae; with 20 pairs of setae (*J1–J5*, *Z1–Z5*, *S1–S5*, and *R1–R5*), eight pairs of distinguishable lyrifissures, and two pairs of distinguishable

gland pores; with a finely denticulate line connecting the bases of setae *J5*. Unsclerotized cuticle along lateral margins of opisthonotal region with five pairs of setae (*R6*, *UR1*, and *UR3–UR5*) and a pair of distinguishable lyrifissures (*Rp*). Measurements of setae: *j1* 24 (23–26), *j2* 19 (17–20), *j3* 20 (18–22), *j4* 19 (17–21), *j5* 18 (17–19), *j6* 21 (20–22), *z1* 15 (14–17), *z2* 20 (19–21), *z3* 20 (19–21), *z4* 21 (20–21), *z5* 22 (20–24), *z6* 22 (21–23), *s1* 17 (15–18), *s2* 20 (18–21), *s3* 21 (19–23), *s4* 21 (19–22), *s5* 23 (22–24), *s6* 23 (21–25), *r2* 21 (20–22), *r3* 28 (27–29), *r4* 19 (18–19), *r5* 18 (18–19), *r6* 16 (16–17), *J1* 22 (21–24), *J2* 23 (20–24), *J3* 22 (21–24), *J4* 24 (23–26), *J5* 17 (15–18), *Z1* 23 (22–25), *Z2* 24 (21–26), *Z3* 24 (22–25), *Z4* 26 (26–27), *Z5* 48 (46–49), *S1* 18 (18–19), *S2* 21 (20–21), *S3* 20 (19–20), *S4* 23 (22–24), *S5* 19 (18–21), *R1* 16 (14–17), *R2* 14 (13–15), *R3* 15 (14–16), *R4* 15 (14–16), *R5* 16 (14–17), *R6* 18 (17–20), *UR1* 14 (13–15), *UR3* 14 (13–16), *UR4* 14 (13–15), *UR5* 14 (13–16); all aciculate and smooth.

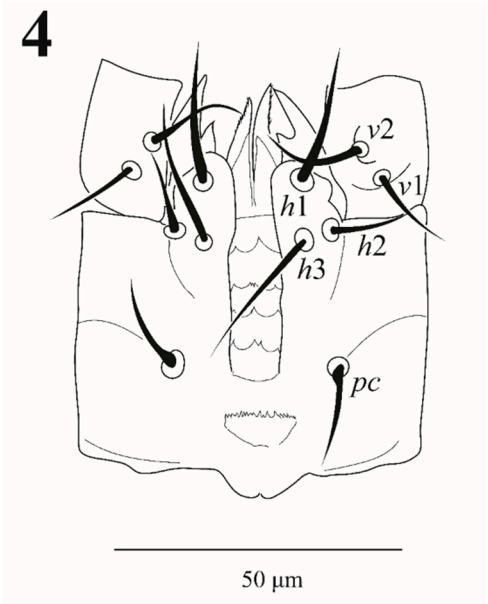


**Figure 4.** *Proctolaelaps ambrosiae* sp. nov., adult female. Hypostome.

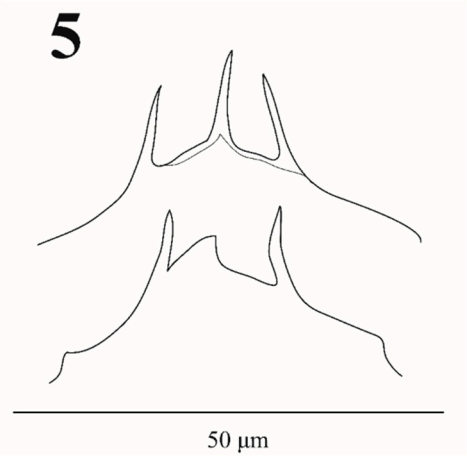


**Figure 5.** *Proctolaelaps ambrosiae* sp. nov., adult female. Epistome.

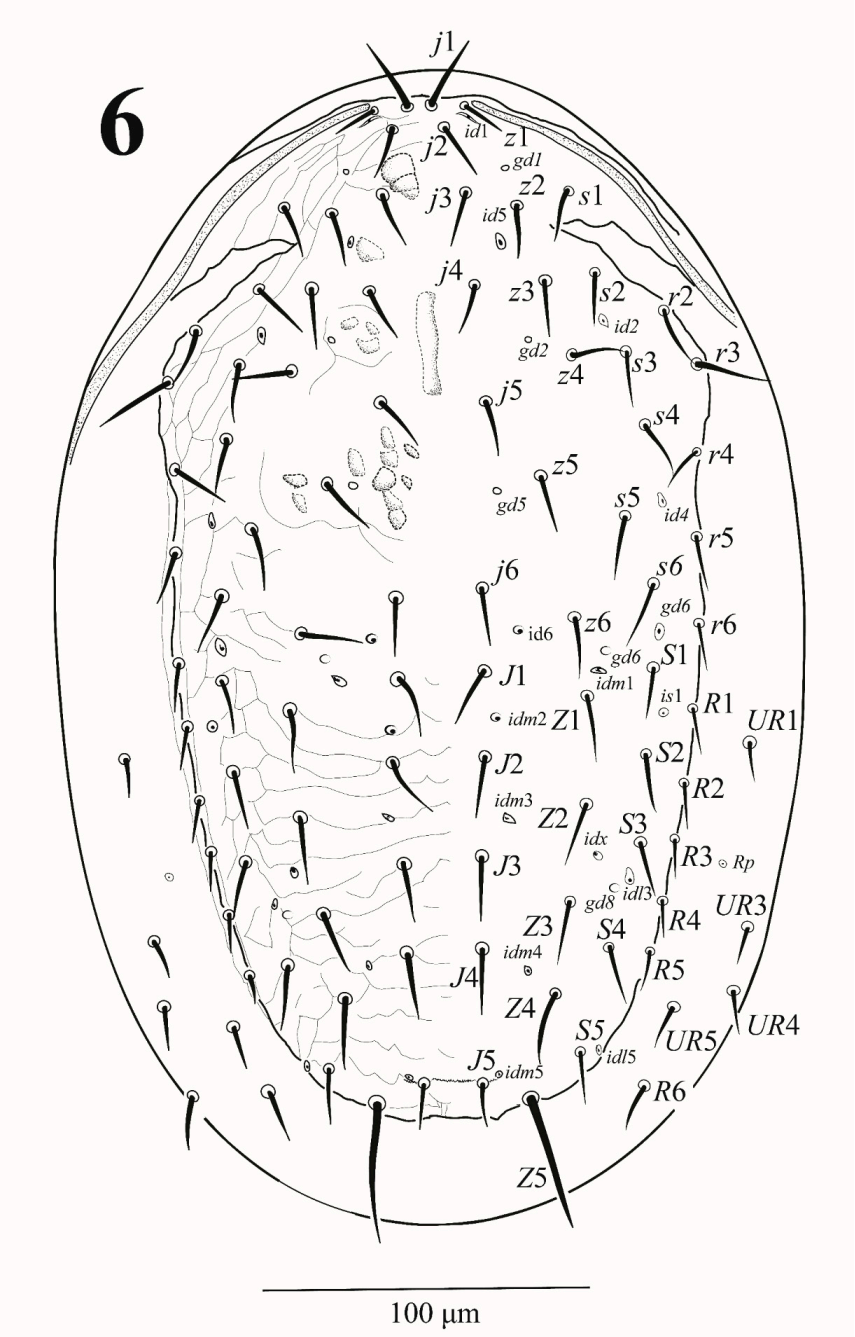


**Figure 6.** *Proctolaelaps ambrosiae* sp. nov., adult female. Dorsal idiosoma.

Venter of idiosoma (Figure 7). Base of tritosternum 12 (11–14) long and 10 (9–11) wide at widest level; laciniae 53 (50–57) long, separate for about 75% of their total length, fimbriate. With a pair of presternal platelets. Sternal shield striated; 107 (97–110) long and 77 (73–81) wide at widest level (next to *st3*); with three pairs of setae (*st1–st3*), and two pairs of lyrifissures (*iv1* and *iv2*); posterior margin about truncate. Metasternal plate irregular, bearing *st4*. Section of endopodal plate laterad coxae III–IV represented by an arched-elongate sclerite. Epigynal shield striated; 169 (158–174) long (including hyaline flap) and 85 (81–87) wide at the level of the posterior margin; with one pair of setae (*st5*); posterior slightly rounded. Lyrifissure *iv5* on unsclerotized cuticle, posterolaterad *st5*. With one transversely curved sclerite between epigynal and anal shields. Anal shield smooth, with a concentric line around the anal opening; 72 (68–75) long and 48 (46–50) wide at widest level; with the circumanal setae and a pair of small glandular openings (*gv3*) on the

edge of the shield, laterad para-anal setae; cribrum composed of two transverse lines of denticles along posterior margin of the shield. Unsclerotized cuticle around anal shield with nine pairs of setae (*Jv1–Jv5*, *Zv1–Zv3*, and *Zv5*), and four pairs of distinguishable lyrifissures. With three pairs of metapodal platelets, the anterior and posterior, smaller; the middle, elongate and punctate. Exopodal plate entire, extending from the posterior margin of coxa II to the posterior margin of coxa IV, fused posteriorly with peritrematic plate at the level of coxa IV, bearing *gv2* right at the margin. Measurements of setae: *st1* 27 (26–28), *st2* 26 (23–27), *st3* 24 (22–25), *st4* 23 (22–24), *st5* 21 (20–21), *Jv1* 19 (17–21), *Jv2* 23 (20–24), *Jv3* 21 (20–21), *Jv4* 21 (20–22), *Jv5* 23 (22–26), *Zv1* 16 (15–17), *Zv2* 19 (18–20), *Zv3* 18 (16–20), para-anal 18 (17–19) and post-anal 34 (33–36); all aciculate and smooth.

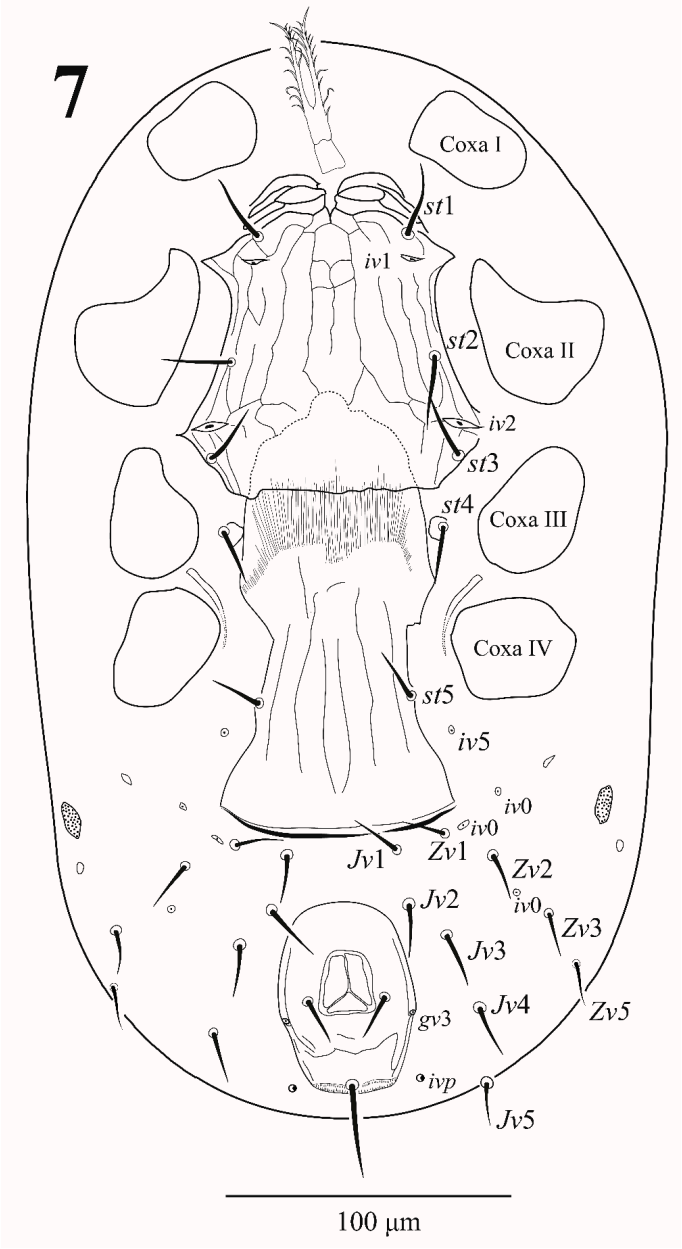


**Figure 7.** *Proctolaelaps ambrosiae* sp. nov., adult female. Ventral idiosoma.

Peritreme and peritrematic strip (Figure 8). Peritreme extends anteriorly to the level of *z1* and posteriorly behind to the level of the anterior margin of coxa IV. Peritrematic plate fused anteriorly with dorsal shield at level of *s1*, and posteriorly with exopodal plate at level of coxa IV, by a narrow bridge; with a lyrifissure (*id3*, sensu Athias-Henriot [41];

*ip2*, sensu Lindquist & Moraza [37]) and a gland pore (*gd3*, sensu Athias-Henriot [41]; *gp1*, sensu Lindquist & Moraza [37]) in the region between coxae II–III, and with a lyrifissure (*ip4*) and a pore (*gp2*) in the connection with the peritrematic bridge and exopodal plate.

Spermathecal apparatus (Figure 9). Slightly variable in shape, apparently because of the different positions in the slide. Spermathecal calyx tubular-shaped, sclerotized.

Legs (Figures 10–13). Leg lengths: I—343 (335–355), II—268 (260–275), III—267 (260–285), and IV—363 (350–370). Chaetotaxy: coxae: I 0-0/1, 0/1-0, II 0-0/1, 0/1-0, III 0-0/1, 0/1-0, IV 0-0/1, 0/0-0; trochanters I 1-1/2, 0/1-1, II 1-1/2, 0/0-1, III 1-1/1, 0/1-1, IV 1-1/1, 0/1-1; femora I 1-2/2, 3/1-2, II 1-3/1, 2/2-1, III 1-2/1, 1/0-1, IV 0-3/1, 1/1-1; genua I 2-2/1, 3/2-3, II 2-3/1, 2/1-2, III 2-2/1, 2/1-1, IV 2-2/1, 3/0-1; tibiae I 2-3/2, 3/1-2, II 2-2/1, 2/1-2, III 1-2/1, 2/1-1, IV 2-2/1, 3/1-1; tarsi I not counted, II–IV 18 setae each. The chaetotaxy of tarsus I has rarely been taken into account, even in the classic work of Evans [38], which deals specifically with the leg chaetotaxy of free-living Mesostigmata. The main reason is apparently due to the large number of setae on this segment and the logistical difficulty of accurately characterizing them. All setae acicular and smooth. All legs with pretarsi, including a pair of claws and a pulvillus with a rounded median lobe.

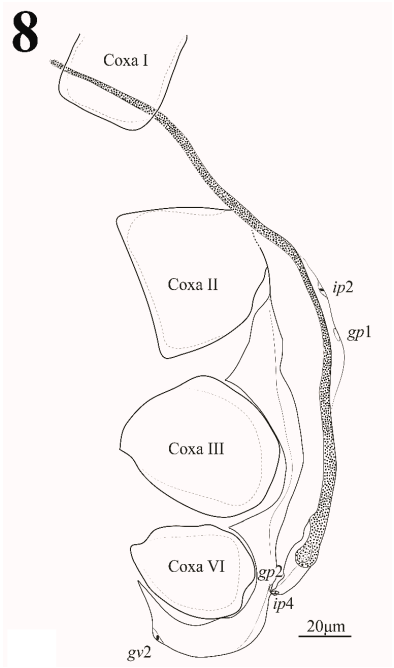


**Figure 8.** *Proctolaelaps ambrosiae* sp. nov., adult female. Peritreme, peritrematic, and exopodal plates.

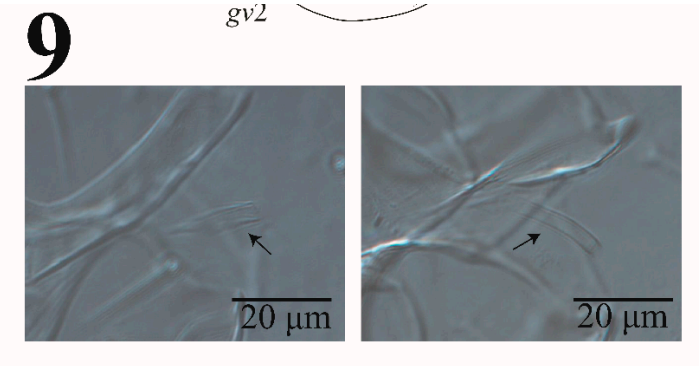


**Figure 9.** *Proctolaelaps ambrosiae* sp. nov., adult female. Sperm access system (arrows) (DIC micrograph).

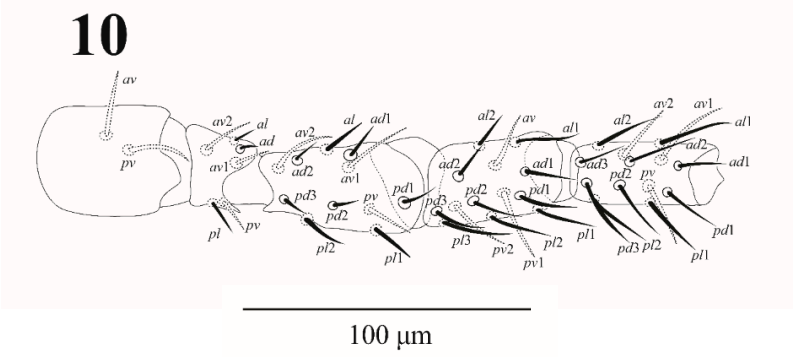


**Figure 10.** *Proctolaelaps ambrosiae* sp. nov., adult female. Leg I (without tarsus and pretarsus).

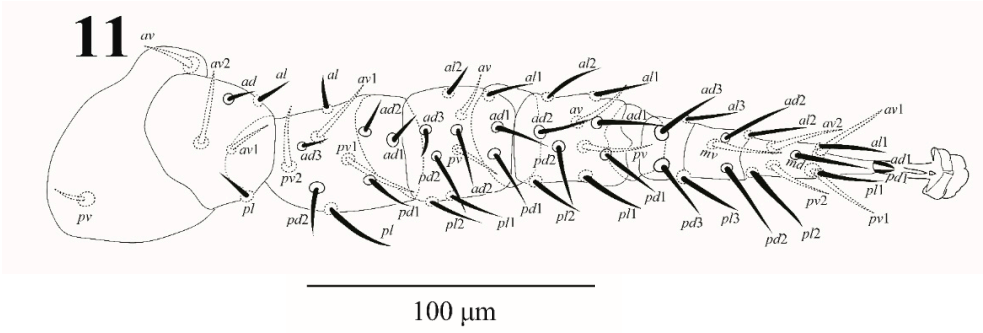


**Figure 11.** *Proctolaelaps ambrosiae* sp. nov., adult female. Leg II.

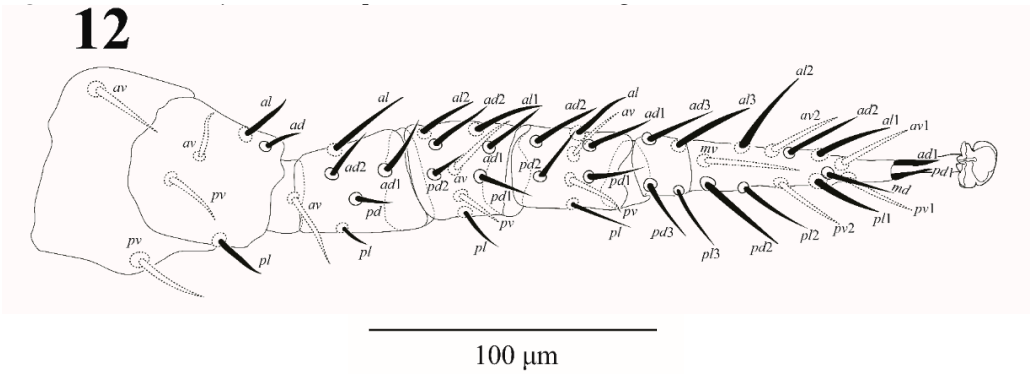


**Figure 12.** *Proctolaelaps ambrosiae* sp. nov., adult female. Leg III.

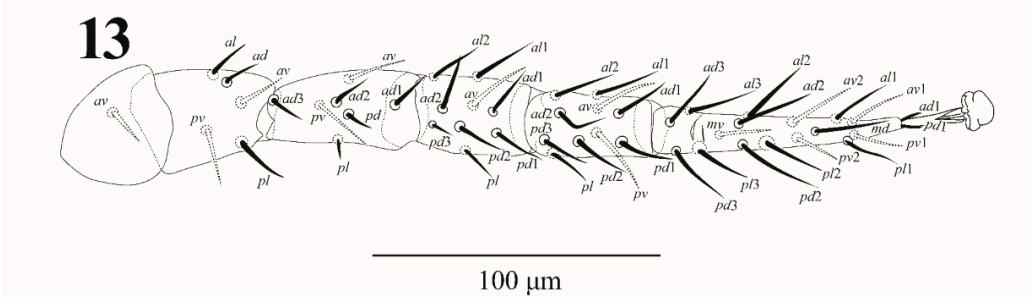


**Figure 13.** *Proctolaelaps ambrosiae* sp. nov., adult female. Leg IV.

MALE. Not found.

### *3.2. Molecular Characterization and Phylogenetic Placement*

Phylogenetic analyses based independently on three molecular markers (28S rDNA, ITS, and COI) consistently supported the recognition of *Proctolaelaps ambrosiae* sp. nov. as

a distinct species-level lineage. Although relationships varied among loci, the placement of this new species relative to closely related taxa within Melicharidae was stable across all individual marker analyses. Sequences obtained from all vouchers were identical for each marker and were therefore collapsed into a single representative haplotype per marker for phylogenetic inference. Newly generated sequences were deposited in GenBank under accession numbers PX985937-PX985942 (28S rDNA), PX984401-PX984406 (ITS), and PX982841-PX982846 (mtCOI) (Table S6).

The 28S ribosomal DNA dataset comprised 30 taxa representing nine Mesostigmata families: Phytoseiidae, Melicharidae, Ologamasidae, Blattisociidae, Digamasellidae, Laelapidae, Podocinidae, Rhodacaridae, and Ascidae. *Pergamasus* sp. (Mesostigmata: Parasitidae) was included as an outgroup to root the analysis. The final 28S alignment contained 426 variable sites, of which 274 were parsimony-informative, and gaps or missing data accounted for 2.27% of the alignment. Pairwise genetic distances calculated from the 28S matrix ranged from 0.001 to 0.71 among this subset (Table S2). The lowest genetic distances for *P. ambrosiae* sp. nov. were observed with *Proctolaelaps* sp. 1 (0.08) and Melicharidae sp. 2 (0.10), whereas the highest distances were observed with *Pergamasus* sp. (outgroup) (0.65) and *Rhodacarellus* sp. (Rhodacaridae) (0.37).

Model selection based on the Bayesian Information Criterion identified the TN93+G substitution model as the best fit for the 28S dataset (lowest BIC = 13,215.205). Maximum likelihood phylogenetic inference under this model, incorporating gamma-distributed rate heterogeneity, recovered a well-resolved topology with branch lengths expressed as substitutions per site. Nodal support was evaluated using 1000 nonparametric bootstrap replicates. The resulting tree recovered a monophyletic *Proctolaelaps* clade nested within Melicharidae, within which *P. ambrosiae* sp. nov. formed an independent lineage with strong bootstrap support (99%), consistent with its morphological placement. No topological instability was observed among strongly supported clades (Figure 14).

The internal transcribed spacer (ITS) dataset comprised 22 Mesostigmata taxa representing seven families: Phytoseiidae, Blattisociidae, Melicharidae, Pachylaelapidae, Laelapidae, Dermanyssidae, and Rhinonyssidae (Figure 15). The ITS alignment contained 549 variable sites, of which 290 were parsimony-informative; gaps and missing data accounted for 32.82% of the final trimmed alignment. Pairwise genetic distances derived from the ITS matrix ranged from 0.00 to 0.65 (Table S3). The lowest divergences for *P. ambrosiae* sp. nov. were recorded with *Lasioseius foliatisetus* Merlin, Castilho & Moraes (Blattisociidae) (0.26) and *Hoploseius oblongus* Mašán & Halliday (Blattisociidae) (0.26). In contrast, the highest divergence was observed with *Rhinonyssus neglectus* Hirst (Rhinonyssidae) (0.4).

Model selection identified the Tamura three-parameter model with gamma-distributed rate heterogeneity (T92+G) as the best-fitting model for the ITS dataset (lowest BIC = 10,392.682). Maximum likelihood inference under this model yielded a well-resolved topology, with nodal support evaluated using 1000 bootstrap replicates. The ITS phylogeny recovered *P. ambrosiae* sp. nov. as an independent lineage within Melicharidae, forming a sister-group relationship with a clade comprising Blattisociidae and Phytoseiidae with moderate bootstrap support (85%). The species was clearly separated from Pachylaelapidae, Laelapidae, Dermanyssidae, and Rhinonyssidae, supporting its phylogenetic placement. This pattern is congruent with the 28S rDNA results and morphological evidence, and no topological instability was observed among well-supported clades (Figure 15).

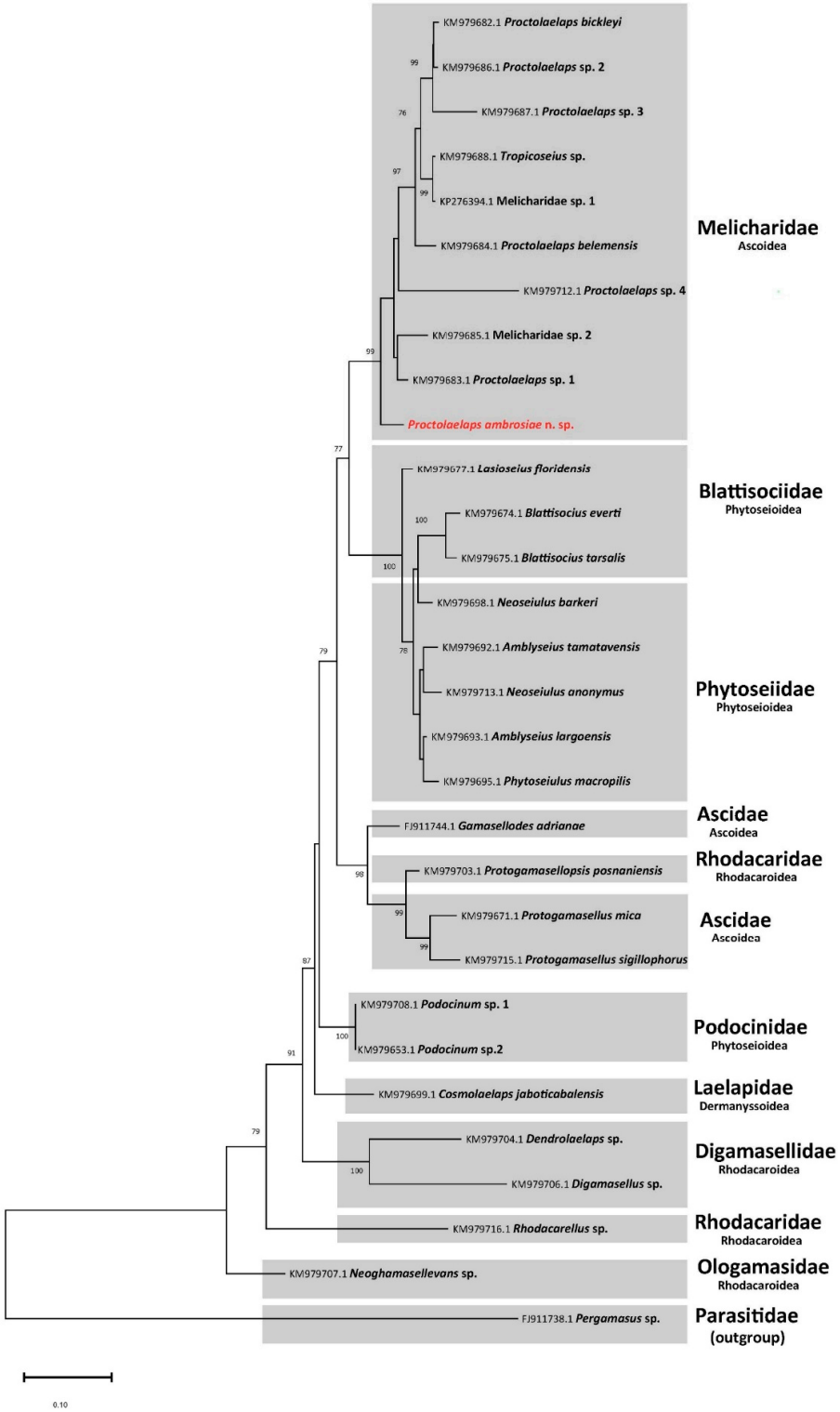


**Figure 14.** Maximum likelihood phylogenetic tree inferred from partial 28S rDNA sequences of 30 Mesostigmata taxa representing nine families: Ascidae, Blattisociidae, Digamasellidae, Laelapidae, Melicharidae, Ologamasidae, Podocinidae, Phytoseiidae, and Rhodacaridae. *Pergamasus* sp. (Parasitidae) was used as the outgroup. The tree was constructed in MEGA 11 using the Tamura-Nei substitution model with gamma-distributed rate heterogeneity (TN93+G). Bootstrap values $\geq$ 70%, based on 1000 replicates, are shown at the corresponding nodes. Branch lengths are proportional to the number of substitutions per site. The new described species, *Proctolaelaps ambrosiae* sp. nov., is highlighted in red.

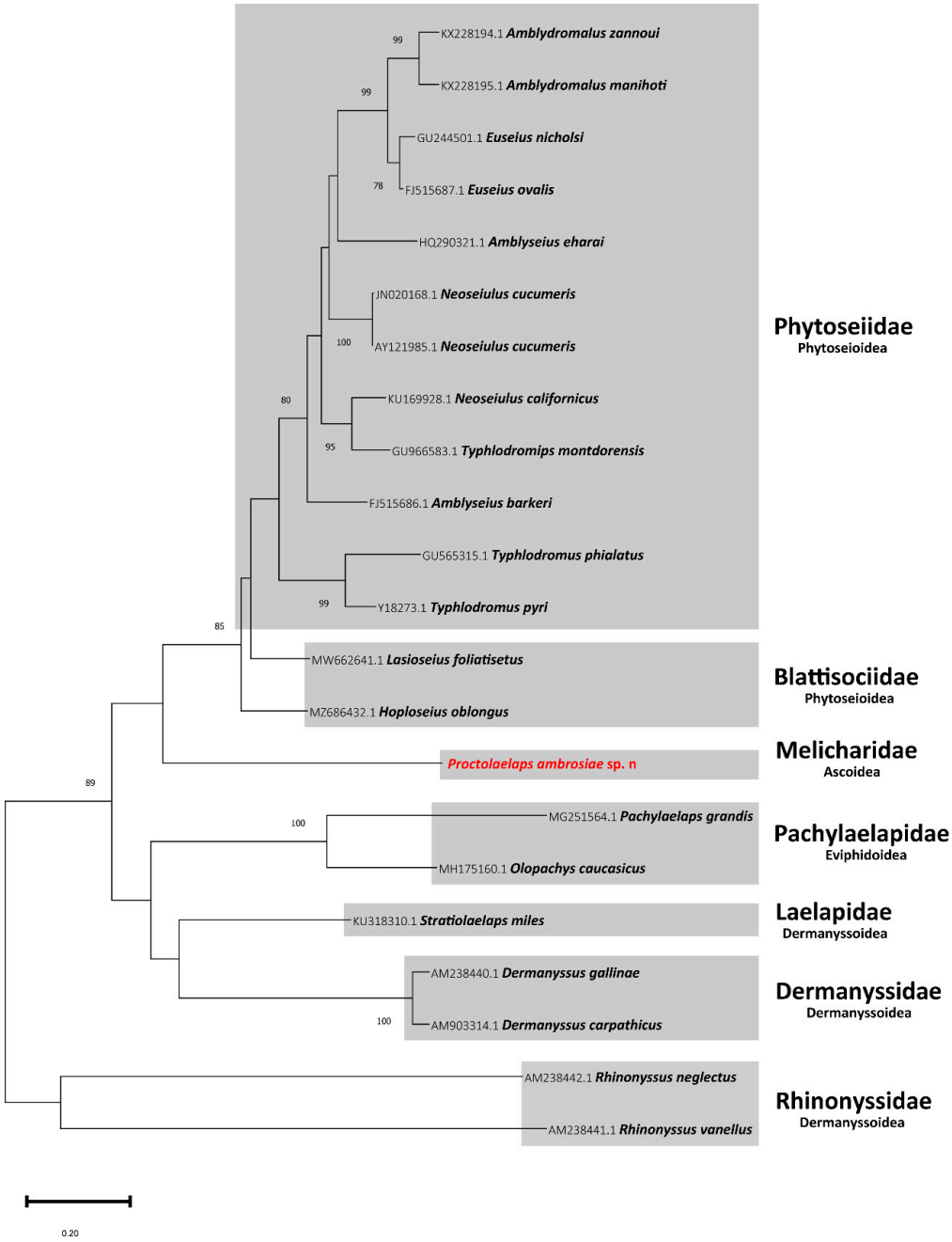


**Figure 15.** Maximum likelihood phylogenetic tree inferred from internal transcribed spacer (ITS) rDNA sequences of 22 Mesostigmata taxa representing seven families: Phytoseiidae, Blattisociidae, Melicharidae, Pachylaelapidae, Laelapidae, Dermanyssidae, and Rhinonyssidae. The tree was constructed in MEGA 11 using the Tamura three-parameter substitution model with gamma-distributed rate heterogeneity (T92+G). Bootstrap support values $\geq$ 70%, based on 1000 replicates, are shown at the corresponding nodes. Branch lengths are proportional to the number of substitutions per site. The new described species, *Proctolaelaps ambrosiae* sp. nov., is highlighted in red.

The mitochondrial cytochrome c oxidase subunit I (COI) dataset comprised 22 Mesostigmata taxa representing eight families: Ascidae, Blattisociidae, Digamasellidae, Laelapidae, Melicharidae, Otopheidomenidae, Rhodacaridae, and Varroidae (Figure 16). The final trimmed COI alignment consisted of 657 nucleotide positions, including 350 variable sites, of which 289 were parsimony-informative. Gaps and missing data accounted for only 0.08% of the dataset. Pairwise genetic distances estimated from the COI matrix ranged from 0.00 to 0.31 (Table S4). For *P. ambrosiae* sp. nov., the lowest genetic distance was observed

with *Proctolaelaps scolyti* Evans (0.11), whereas the highest divergence was recorded with *Varroa destructor* Anderson & Trueman (Varroidae) (0.28).

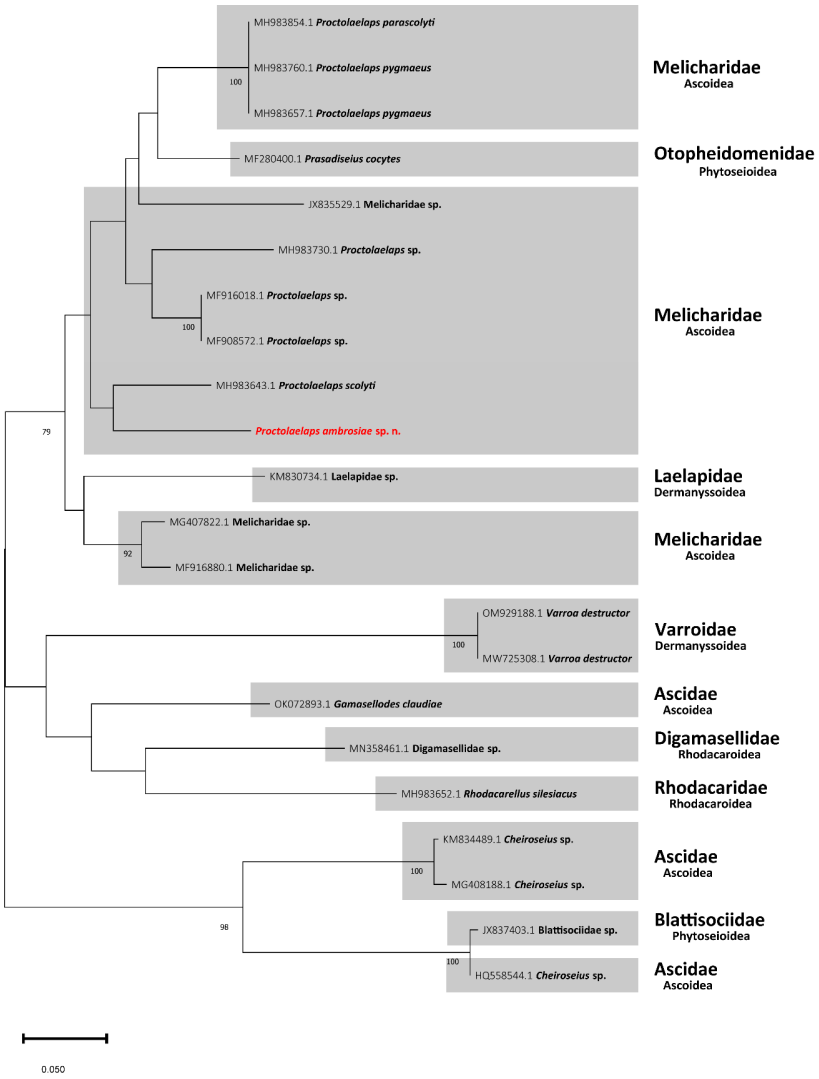


**Figure 16.** Maximum likelihood phylogenetic tree inferred from mitochondrial cytochrome c oxidase subunit I (COI) sequences of 22 Mesostigmata taxa representing eight families: Ascidae, Blattisociidae, Digamasellidae, Laelapidae, Melicharidae, Otopheidomenidae, Rhodacaridae, and Varroidae. The analysis was conducted in MEGA version 11 under the Tamura two-parameter substitution model with gamma-distributed rate heterogeneity (T92+G). Bootstrap support values $\geq$ 70%, based on 1000 replicates, are shown at the corresponding nodes. Branch lengths are proportional to the number of substitutions per site. The new described species, *Proctolaelaps ambrosiae* sp. nov., is highlighted in red.

Model selection based on the BIC identified the Tamura two-parameter model with gamma-distributed rate heterogeneity (T92+G) as the best-fitting model for the COI dataset (lowest BIC = 11,097.437). Maximum-likelihood inference under this model incorporated gamma-distributed rate variation (shape parameter = 0.80; five rate categories). Nodal support was assessed using 1000 bootstrap replicates, and branch lengths are expressed as substitutions per site. The COI phylogeny recovered *P. ambrosiae* sp. nov. as a well-supported member of the *Proctolaelaps* clade within Melicharidae, consistent with results from nuclear markers and morphological evidence. Relationships among deeper family-level lineages were generally weakly supported and are therefore interpreted with caution (Figure 16).

*Type specimens*. Holotype: Adult female, slide-mounted in Hoyer's medium, collected from an adult ambrosia beetle, *Xyleborinus saxesenii* (Ratzeburg) (Scolytinae: Xyleborini), infesting avocado (*Persea americana* Mill.; Lauraceae) at Homestead (25°30′44.24″ N, 80°31′10.03″ W), Miami-Dade County, FL, USA, in 15. iii. 2023, coll. M. M. Berto; deposited in the Florida State Collection of Arthropods, Gainesville, FL, USA (FSCA). Paratypes: Eleven adult females, slide-mounted in Hoyer's medium, collected from adults of ambrosia beetles *X. saxesenii*, *Xyleborus affinis* Eichhoff (Scolytinae: Xyleborini), or from galleries of unidentified xyleborini ambrosia beetles associated with avocado, from the same date and locality as the holotype. All types collected by M. M. Berto. Holotype and four paratypes deposited at Florida State Collection of Arthropods, Gainesville, FL, USA (FSCA); five paratypes deposited at Tropical Fruit Entomology Laboratory, University of Florida's Tropical Research and Education Center, Homestead, FL, USA (UF-Tropento); and two paratypes deposited at Mite Reference Collection of the Departamento de Entomologia e Acarologia, Escola Superior de Agricultura Luiz de Queiroz (ESALQ), Universidade de São Paulo, Piracicaba, São Paulo State, Brazil (MZLQ). Full specimen-level provenance, host association, and repository information for the holotype and paratype series are provided in Supplementary Table S5.

*Etymology*. The name *ambrosiae* refers to the association of the new species with the ambrosia beetles.

*Remarks*. *Proctolaelaps ambrosiae* Berto & Castilho sp. nov. is similar to species of the *hystrix* species group [*P. appendiculatus* Mašán; *P. aurora* (Vitzthum); *P. australis* Stone; *P. citri* Chant; *P. coffeae* Karg & Rodriguez; *P. conifericola* Mašán; *P. coralifer* Mašán; *P. fagi* Mašán; *P. fiseri* Samšiňák; *P. fusifer* Mašán; *P. holmi* Halliday; *P. hystricoides* Lindquist & Hunter; *P. hystrix* (Vitzthum); *P. laeviusculus* Mašán; *P. novaeguineae* (Oudemans); *P. ovianalis* Karg; *P. pcolai* Mašán; *P. populi* Mašán; and *P. trirami* Karg] by the multidentate fixed digit of the chelicerae, the presence of a triramous epistome, subcapitular setae similar in thickness, and the absence of the opisthogastric setae *Sv2* and the third pair of sternal lyrifissures (*iv3*) [48]. The new species can be distinguished from these members of the *hystrix* group, especially by the following combination of characters: 43 pairs of dorsal shield setae (opisthonotal region has five pairs of marginal setae, *R1–R5*); and palp tarsal claw with the bulbous base.

Among the species in the *hystrix* species group, *P. ambrosiae* sp. nov. is most similar to *P. appendiculatus*, *P. coffeae*, *P. fagi*, *P. fiseri*, *P. hystricoides*, and *P. populi* mainly by the dorsal setae relatively short (*J1–J3* usually not reaching bases of following setae). Table S7 synthesizes the available literature and diagnostic characters supporting the separation of these seven species, including the new species described herein.

The close association of *P. ambrosiae* sp. nov. with *P. scolyti* in COI-based analyses likely reflects the limited taxon sampling currently available for *Proctolaelaps* in GenBank rather than close morphological affinity. For the COI marker, the nucleotide composition of *P. ambrosiae* sp. nov. is most similar to that reported for *P. scolyti*. However, *P. scolyti* was not assigned to any *Proctolaelaps* species group [48] and differs morphologically from species of the *hystrix* group by having an anterior epistome margin broadly convex, with a rounded or slightly tricuspid apex that is irregularly serrate or denticulate, and by the presence of opisthogastric setae *Sv2*. Furthermore, *P. scolyti* differs from *P. ambrosiae* sp. nov. in possessing a fixed cheliceral digit with approximately 15 teeth, a fully reticulate dorsal shield (including the area between setae *j5*, *z5*, and *j6*), a presternal area with fine transverse striations and weakly sclerotized platelets, and 15 pairs of opisthogastric setae on the unsclerotized cuticle, including *R5* and *Sv2* (with seta *UR1* absent). To date, no COI sequences of species belonging to the *hystrix* group are available in GenBank.

## 4. Discussion

The genus *Proctolaelaps* is recognized for its possible role in biological control and its frequent association with wood-boring insects, particularly bark beetles [13,17]. Species of this genus are commonly encountered in beetle galleries, where they may engage in phoretic relationships or function as facultative predators of eggs, larvae, or other microarthropods occupying the same microhabitats [8,14]. These ecological interactions suggest a potential regulatory influence on beetle populations, either through direct predation on immature stages or by disrupting fungus-farming activities that are critical to the reproductive success of many wood-boring species [21,24,49].

The present study provides the first formal documentation of a *Proctolaelaps* species associated with xyleborini ambrosia beetles and their galleries, thereby extending the genus's known ecological range beyond bark beetle systems. Ambrosia beetles excavate galleries within the xylem of trees, creating structurally stable microhabitats suitable for mite colonization. The recovery of *P. ambrosiae* sp. nov. from ambrosia beetle galleries indicates that this species can persist in these environments.

Additional support for this ecological association is provided by the successful establishment and maintenance of a laboratory colony of *P. ambrosiae* sp. nov. originating from field-collected individuals [28]. Under controlled conditions, the species survived and reproduced across multiple generations when maintained using a standardized rearing protocol. This capacity for sustained reproduction outside the immediate presence of the beetle host suggests that *P. ambrosiae* sp. nov. is not an obligate phoretic associate, but rather a facultative gallery-dwelling species capable of exploiting resources within the beetle microhabitat. Such life-history flexibility is consistent with patterns reported for other melicharid mites associated with wood-boring insects [2].

In addition to ecological evidence, molecular data further support the distinctiveness of *P. ambrosiae* sp. nov. Molecular tools have become increasingly important for identifying predatory mites and resolving taxonomic boundaries. To date, 162 molecular sequences attributed to *Proctolaelaps* have been deposited in GenBank®, of which approximately 74% correspond to the COI gene. However, most of these sequences are not linked to specimens identified to species level, thereby limiting their taxonomic utility.

In the 28S rDNA phylogeny, *P. ambrosiae* sp. nov. was recovered as an independent lineage within a well-supported Melicharidae clade (bootstrap support = 99%), consistent with the current morphological classification of the family proposed by Moraza and Lindquist [50]. Although explicit genetic distance thresholds for species delimitation within *Proctolaelaps* have not yet been established, the relatively low pairwise genetic distances observed between *P. ambrosiae* sp. nov. and other *Proctolaelaps* representatives in the 28S dataset (0.08–0.21) support its recognition as a distinct species within the genus. At higher taxonomic levels, Blattisociidae and Phytoseiidae, both belonging to Phytoseioidea, were recovered as adjacent but clearly distinct clades. In contrast, taxa assigned to Ascidae (Ascoidea) were placed more distantly and showed affinities with representatives of Rhodacaroidea, reflecting limited resolution at deeper nodes.

Previous molecular analyses have similarly reported weak support for higher-level relationships within Ascoidea. For example, Sourassou et al. [51] observed low bootstrap support for this superfamily, suggesting that both molecular data and the morphological framework proposed by Moraza and Lindquist [50] face limitations in resolving interfamily relationships. These results underscore the need for expanded taxon sampling and the inclusion of additional molecular markers to improve phylogenetic resolution at deeper hierarchical levels.

For the ITS marker, the availability of Melicharidae sequences in public databases remains limited, restricting direct intrafamilial comparisons. Despite this limitation, the ITS

phylogeny clearly supported the molecular distinctiveness of *P. ambrosiae* sp. nov. relative to other Mesostigmata families. Most published benchmarks for ITS-based interspecific divergence in Mesostigmata derive from Phytoseiidae, where divergences of approximately 6% have been reported among closely related species [52–54]. In contrast, the substantially higher ITS divergences observed between *P. ambrosiae* sp. nov. and other mesostigmatid taxa in this study (26–40%) are consistent with species-level separation. The ITS sequence generated here represents an important reference point that may facilitate future efforts to define divergence thresholds within *Proctolaelaps* and Melicharidae.

Among the molecular markers analyzed, COI was the most widely represented for *Proctolaelaps* and Melicharidae in the Barcode of Life Data System (BOLD), whereas reference sequences for 28S rDNA and ITS were comparatively scarce. Despite its broad availability, COI did not resolve family-level relationships within Mesostigmata with strong support, as evidenced by low bootstrap values at deeper nodes. This pattern highlights the importance of critically evaluating COI sequences and their associated morphological identifications in public databases, as misidentifications or insufficient taxonomic validation can substantially reduce their phylogenetic utility [55,56]. Nevertheless, the COI interspecific divergences observed among *Proctolaelaps* species in this study (11–16%) fall within ranges reported for other mesostigmatid families. Comparable divergence values have been documented in Laelapidae (12.5–34.4%) [57] and Phytoseiidae [58]. However, previous studies have also emphasized that misidentified specimens or contaminated sequences may artificially inflate divergence estimates. Such issues likely contribute to broad divergence ranges reported in public repositories and further underscore the necessity of integrative approaches that combine morphological and molecular data. Overall, the phylogenetic patterns recovered in this study support a stable interpretation of species boundaries and interspecific relationships within *Proctolaelaps* and Melicharidae. Differences in phylogenetic resolution among markers are more plausibly attributed to incomplete taxon sampling and gaps in available reference data than to conflicts with morphological evidence. These findings reinforce the importance of detailed species descriptions supported by vouchered material and multilocus datasets for advancing the systematics of mesostigmatid mites.

## 5. Conclusions

The integrative taxonomic approach applied here, combining detailed morphological analyses with multiple molecular markers, supports the recognition of *Proctolaelaps ambrosiae* sp. nov. and underscores the need for improved molecular reference libraries for Melicharidae. The recovery of *P. ambrosiae* sp. nov. from xyleborine ambrosia beetle species and their galleries in avocado systems indicates that this new species exploits resources in the ambrosia beetle gallery environments. Although its precise ecological role remains unresolved, these findings provide a foundation for future investigations into the mite–beetle–fungus–plant multipartite symbiotic system.

**Supplementary Materials:** The following supporting information can be downloaded at: https://www.mdpi.com/article/10.3390/arthropoda4010003/s1, Table S1: GenBank sequences used in Phylogenetic Analysis with corresponding Accession numbers.; Table S2: Summary of pairwise genetic distances among 30 Mesostigmata taxa based on 28S rDNA sequences; Table S3: Summary of pairwise genetic distances among 22 Mesostigmata taxa based on ITS rDNA sequences; Table S4: Summary of pairwise genetic distances among 22 Mesostigmata taxa based on mtCOI sequences; Table S5: Type material of *Proctolaelaps ambrosiae* sp. nov., including holotype and paratype specimens with permanent identifiers, provenance, and repository information; Table S6: Voucher–sequence correspondence for *Proctolaelaps ambrosiae* sp. nov., linking molecular voucher specimens to GenBank accession numbers for 28S rRNA, ITS, and COI markers; Table S7: Comparative diagnostic

characters separating *Proctolaelaps ambrosiae* sp. nov. from morphologically similar species of the hystrix group.

**Author Contributions:** Conceptualization, M.M.B. and D.C.; methodology, M.M.B., A.D.T. and R.d.C.C.; formal analysis, M.M.B., A.D.T., D.C., and R.d.C.C.; investigation, M.M.B., A.D.T., R.d.C.C. and D.C.; resources, R.d.C.C. and D.C. writing—original draft preparation, M.M.B.; writing—review and editing, M.M.B., A.D.T., A.R.d.A.B., D.C. and R.d.C.C.; funding acquisition, D.C. All authors have read and agreed to the published version of the manuscript.

**Funding:** In part, this research was supported by the National Plant Disease Recovery System under USDA in-house project (5010-22410-024-00-D), USDA ARS-UF Non-Assistance Cooperative Agreement No.58-6038-3-002, and USDA NIFA grant 2024-51181-43302.

**Institutional Review Board Statement:** Ethical review and approval were not required for this study because it involved only non-vertebrate invertebrates (mites, Acari) collected from agricultural systems. Research on free-living invertebrates is exempt from Institutional Review Board (IRB) and Institutional Animal Care and Use Committee (IACUC) oversight under U.S. federal regulations and Florida state law. No humans, vertebrate animals, or protected species were involved.

**Data Availability Statement:** The original contributions presented in this study are included in the article and Supplementary Material. Further inquiries can be directed to the corresponding author.

**Acknowledgments:** We thank Armando Padilla for helping with the mite and ambrosia beetle collection. We also thank the Florida Avocado Administrative Committee for facilitating access to the avocado groves visited during this work.

**Conflicts of Interest:** The authors declare no conflicts of interest. The funders had no role in the design of the study; in the collection, analyses, or interpretation of data; in the writing of the manuscript; or in the decision to publish the results.

## References

1. Moraes, G.J.; Britto, E.P.J.; Mineiro, J.L.C.; Halliday, B. Catalogue of the mite families Ascidae, Blattisociidae and Melicharidae (Acari: Mesostigmata). *Zootaxa* **2016**, *4112*, 1–299. [CrossRef]
2. Santos, J.C.; Demite, P.R.; Moraes, G.J. Melicharidae Database. 2026. Available online: http://www.lea.esalq.usp.br/acari/melicharidae (accessed on 4 February 2026).
3. Ueckermann, E.A.; Faraji, F.; Simoni, S.; Guidi, S.; Moraes, G.J.; Abo-Shnaf, R. *Proctolaelaps* mites from Africa. *Int. J. Acarol.* **2023**, *49*, 8–23. [CrossRef]
4. Gómez-Moya, C.A.; Martin, J.P.I.; Feliz Lebrón, A.O.F.; Moraes, G.J. A new species of *Proctolaelaps* Berlese (Acari: Mesostigmata: Melicharidae) from the Dominican Republic. *Acarologia* **2023**, *63*, 856–866. [CrossRef]
5. Wang, H.; Abo-Shnaf, R.; Wang, Y.; Xie, L.; Yan, Y. A new species and a new record of *Proctolaelaps* associated with insects. *Syst. Appl. Acarol.* **2025**, *30*, 121–134. [CrossRef]
6. Abo-Shnaf, R.I.; Moraes, G.J. *Proctolaelaps* species (Acari: Mesostigmata: Melicharidae) from Egypt, with description of a new species and complementary descriptions of other five species. *Zootaxa* **2016**, *4162*, 479–503. [CrossRef] [PubMed]
7. Guerra, T.J.; Romero, G.Q.; Costa, J.C.; Lofego, A.C.; Benson, W.W. Phoretic dispersal on bumblebees by bromeliad flower mites (Mesostigmata: Melicharidae). *Insectes Soc.* **2012**, *59*, 11–16. [CrossRef]
8. Lindquist, E.E.; Hunter, P.E. Some mites of the genus *Proctolaelaps* Berlese (Acarina: Blattisociidae) associated with forest insect pests. *Can. Entomol.* **1965**, *97*, 15–32. [CrossRef]
9. Krantz, G.W.; Poinar, G.O., Jr. Mites, nematodes and the multimillion dollar weevil. *J. Nat. Hist.* **2004**, *38*, 135–141. [CrossRef]
10. O'Connor, B.M.; Colwell, R.K.; Naeem, S. Flower mites of Trinidad II. The genus Proctolaelaps (Acari: Ascidae). *Great Basin Nat.* **1991**, *51*, 348–376.
11. Salmane, I. Mesostigmata mites of wood-related microhabitats in Latvia. *Latv. Entomol.* **2007**, *44*, 69–86.
12. Moser, J.C.; Konrad, H.; Blomquist, S.R.; Kirisits, T.; Gebhardt, T.M.; Müller, W.H.J. Do mites phoretic on elm bark beetles contribute to the transmission of Dutch elm disease? *Naturwissenschaften* **2010**, *97*, 219–227. [CrossRef] [PubMed]
13. Moraes, G.J.; Venancio, R.; Santos, V.L.V.; Paschoal, A.D. Potential of Ascidae, Blattisociidae and Melicharidae (Acari: Mesostigmata) as biological control agents. In *Prospects for Biological Control of Plant Feeding Mites and Other Harmful Organisms*; Carrillo, D., Moraes, G.J., Peña, J.E., Eds.; Springer: Cham, Switzerland, 2015; pp. 33–75. [CrossRef]

14. Trach, V.A.; Khaustov, A.A. Mites of the genus *Proctolaelaps* associated with bark beetles in Asian Russia. *Acarina* **2017**, *25*, 151–163. [CrossRef]
15. McGraw, J.R.; Farrier, M.H. Mites of the superfamily Parasitoidea (Acarina: Mesostigmata) associated with *Dendroctonus* and *Ips* (Coleoptera: Scolytidae). *N.C. Agric. Exp. Stn. Tech. Bull.* **1969**, *192*, 162.
16. Moser, J.C.; Roton, L.M. Mites associated with southern pine bark beetles in Louisiana. *Can. Entomol.* **1971**, *103*, 1775–1798. [CrossRef]
17. Vissa, S.; Hofstetter, R.W. The role of mites in bark and ambrosia beetle–fungal interactions. In *Insect Physiology and Ecology*; Shields, V.D.C., Ed.; InTech: Rijeka, Croatia, 2017; pp. 135–156. [CrossRef]
18. Khaustov, A.; Klimov, P.; Trach, V.; Bobylev, A.; Salavatulin, V.; Khaustov, V.; Tolstikov, A. Review of mites (Acari) associated with the European spruce bark beetle, *Ips typographus* (Coleoptera: Curculionidae: Scolytinae) in Asian Russia. *Acarina* **2018**, *26*, 3–79. [CrossRef]
19. Cruz, L.F.; Rocio, S.A.; Duran, L.G.; Menocal, O.; Garcia-Avila, D.J.; Carrillo, D. Developmental biology of *Xyleborus bispinatus* (Coleoptera: Curculionidae) reared on an artificial medium and fungal cultivation of symbiotic fungi in the beetle's galleries. *Fungal Ecol.* **2018**, *35*, 116–126. [CrossRef]
20. Menocal, O.G.; Kendra, P.E.; Padilla, A.; Cardoso Chagas, P.; Alves Chagas, E.; Crane, J.H.; Carrillo, D. Influence of canopy cover and meteorological factors on the abundance of bark and ambrosia beetles in avocado orchards affected by laurel wilt. *Agronomy* **2022**, *12*, 547. [CrossRef]
21. Cruz, L.F.; Menocal, O.; Kendra, P.E.; Carrillo, D. Phoretic and internal transport of *Raffaelea lauricola* by different species of ambrosia beetles associated with avocado trees. *Symbiosis* **2021**, *84*, 151–161. [CrossRef]
22. Menocal, O.G.; Cruz, L.F.; Kendra, P.E.; Berto, M.; Carrillo, D. Flexibility in the ambrosia symbiosis of *Xyleborus bispinatus*. *Front. Microbiol.* **2023**, *14*, 1110474. [CrossRef]
23. Carrillo, D.; Duncan, R.E.; Ploetz, J.N.; Campbell, A.F.; Ploetz, R.C.; Peña, J.E. Lateral transfer of a phytopathogenic symbiont among native and exotic ambrosia beetles. *Plant Pathol.* **2014**, *63*, 54–62. [CrossRef]
24. Carrillo, D.; Cruz, L.F.P.; Kendra, P.E.; Narvaez, T.; Montgomery, W.; Monterroso, A.; De Grave, C.; Cooperband, M.F. Distribution, pest status and fungal associates of *Euwallacea* nr. *fornicatus* in Florida avocado groves. *Insects* **2016**, *7*, 55. [CrossRef]
25. Kanzaki, N.; Giblin-Davis, R.M.; Carrillo, D.; Duncan, R.E.; Gonzalez, R. *Bursaphelenchus penai* n. sp. (Tylenchomorpha: Aphelenchoididae), a phoretic associate of ambrosia beetles (Coleoptera: Scolytinae) from avocado in Florida. *Nematology* **2014**, *16*, 683–693. [CrossRef]
26. Kanzaki, N.; Giblin-Davis, R.M.; Gonzalez, R.; Duncan, R.E.; Carrillo, D. Description of *Ruehmaphelenchus juliae* n. sp. (Tylenchina: Aphelenchoididae) isolated from an ambrosia beetle, *Xylosandrus crassiusculus*, from South Florida. *Nematology* **2015**, *17*, 639–653. [CrossRef]
27. Khaustov, A.A.; Berto, M.; Carrillo, D. A new species of *Brasilopsis* and redescription of *Acarothorectes curculionium* (Acari: Pygmephoridae) associated with ambrosia beetles (Coleoptera: Scolytinae) from the USA. *Syst. Appl. Acarol.* **2022**, *27*, 1648–1662. [CrossRef]
28. Berto, M.M.; Hajihassani, A.; Carrillo, D. Rearing phoretic mites associated with wood-boring insects. *J. Vis. Exp.* **2025**, *223*, e69039. [CrossRef]
29. Berto, M.M.; Cruz, L.F.; Avery, P.B.; Cloonan, K.R.; Dunlap, C.; Carrillo, D. Beyond phoresy: Interactions between *Histiogaster arborsignis* (Acari: Acaridae), ambrosia beetles and their fungal symbionts in Florida avocados. *Symbiosis* **2025**, *96*, 91–104. [CrossRef]
30. Lindquist, E.E. New species of Ascidae (Acarina: Mesostigmata) associated with forest insect pests. *Can. Etomol.* **1971**, *103*, 919–942. [CrossRef]
31. Biswas, T.; Yuvaraj, J.K.; Hansson, B.S.; Löfstedt, C.; Anderbrant, O.; Andersson, M.N. Characterization of olfactory sensory neurons in the striped ambrosia beetle *Trypodendron lineatum*. *Front. Physiol.* **2023**, *14*, 1155129. [CrossRef] [PubMed]
32. Lindgren, B.S. A multiple funnel trap for scolytid beetles (Coleoptera). *Can. Entomol.* **1983**, *115*, 299–302. [CrossRef]
33. Menocal, O.G.; Kendra, P.E.; Montgomery, W.S.; Crane, J.H.; Carrillo, D. Vertical distribution and daily flight periodicity of ambrosia beetles (Coleoptera: Curculionidae) in Florida avocado orchards affected by laurel wilt. *J. Econ. Entomol.* **2018**, *111*, 1190–1196. [CrossRef] [PubMed]
34. Lindquist, E.E.; Krantz, G.W.; Walter, D.E. Order Mesostigmata. In *A Manual of Acarology*, 3rd ed.; Krantz, G.W., Walter, D.E., Eds.; Texas Tech University Press: Lubbock, TX, USA, 2009; pp. 124–232.
35. Lindquist, E.E.; Evans, G.O. Taxonomic concepts in the Ascidae, with a modified setal nomenclature for the idiosoma of the Gamasina (Acarina: Mesostigmata). *Mem. Entomol. Soc. Can.* **1965**, *97*, 5–66. [CrossRef]
36. Lindquist, E.E. Some observations on the chaetotaxy of the caudal body region of gamasine mites (Acari: Mesostigmata), with a modified notation for some ventrolateral body setae. *Acarologia* **1994**, *35*, 323–326.
37. Lindquist, E.E.; Moraza, M.L. A new genus of flower-dwelling melicharid mites (Acari: Mesostigmata: Ascoidea) phoretic on bats and insects in Costa Rica and Brazil. *Zootaxa* **2008**, *1685*, 1–37. [CrossRef]

38. Evans, G.O. Observations on the chaetotaxy of the legs in the free-living Gamasina (Acari: Mesostigmata). *Bull. Nat. Hist. Mus. Zool.* **1963**, *10*, 277–303. [CrossRef]
39. Evans, G.O. Some observations on the chaetotaxy of the pedipalps in the Mesostigmata (Acari). *Ann. Mag. Nat. Hist.* **1963**, *6*, 513–527. [CrossRef]
40. Athias-Henriot, C. La divergence néotaxique des Gamasides (Arachnides). *Bull. Sci. Bourgogne* **1971**, *28*, 93–106.
41. Athias-Henriot, C. Nouvelles notes sur les Amblyseiini. II—Le relevé organotaxique de la face dorsale d'adulte (Gamasides Protoadeniques, Phytoseiidae). *Acarologia* **1975**, *17*, 20–29.
42. Dowling, A.P.G.; Ochoa, R.; Beard, J.J.; Welbourn, W.C.; Ueckermann, E.A. Phylogenetic investigation of the genus *Raoiella* (Prostigmata: Tenuipalpidae): Diversity, distribution, and world invasions. *Exp. Appl. Acarol.* **2012**, *57*, 257–269. [CrossRef]
43. Dowling, A.P.G.; O'Connor, B.M. Phylogenetic relationships within the suborder Dermanyssina (Acari: Parasitiformes) and a test of dermanyssoid monophyly. *Int. J. Acarol.* **2010**, *36*, 299–312. [CrossRef]
44. Tixier, M.-S.; Okassa, M.; Kreiter, S. An integrative morphological and molecular diagnostics for *Typhlodromus pyri* (Acari: Phytoseiidae). *Zool. Scr.* **2011**, *41*, 68–78. [CrossRef]
45. Folmer, O.; Black, M.; Hoeh, W.; Lutz, R.; Vrijenhoek, R. DNA primers for amplification of mitochondrial cytochrome c oxidase subunit I from diverse metazoan invertebrates. *Mol. Mar. Biol. Biotechnol.* **1994**, *3*, 294–299.
46. Tamura, K.; Stecher, G.; Kumar, S. MEGA11: Molecular evolutionary genetics analysis version 11. *Mol. Biol. Evol.* **2021**, *38*, 3022–3027. [CrossRef]
47. Tamura, K.; Nei, M. Estimation of nucleotide substitutions in mitochondrial DNA. *Mol. Biol. Evol.* **1993**, *10*, 512–526.
48. Cruz, L.F.P.; Menocal, O.G.; Dunlap, C.; Cooperband, M.F.; Cloonan, K.R.; Tabanca, N.; Carrillo, D. Insights on the tea shot hole borer (Coleoptera: Curculionidae) symbiotic associations. *Front. Microbiol.* **2025**, *16*, 1589710. [CrossRef]
49. Mašán, P. The family Melicharidae (Acari, Mesostigmata) in Slovakia, with description of new species, annotated faunal synopsis and identification keys of species from Europe. *Zootaxa* **2022**, *5172*, 1–449. [CrossRef]
50. Moraza, M.L.; Lindquist, E.E. Systematics and biology of mites associated with neotropical hispine beetles. *Zootaxa* **2015**, *3931*, 301–351. [CrossRef]
51. Sourassou, N.F.; Moraes, G.J.; Delalibera, I.; Corrêa, A.S. Phylogenetic analysis of Ascidae sensu lato. *Syst. Appl. Acarol.* **2015**, *20*, 225–240. [CrossRef]
52. Tixier, M.-S.; Kreiter, S.; Ferragut, F.; Cheval, B. The suspected synonymy of *Kampimodromus hmiminai* and *Kampimodromus adrianae* (Acari: Phytoseiidae): Morphological and molecular investigations. *Can. J. Zool.* **2006**, *84*, 1216–1222. [CrossRef]
53. Kanouh, M.; Tixier, M.-S.; Guichou, S.; Cheval, B.; Kreiter, S. Two synonymy cases within the genus *Neoseiulella* (Acari: Phytoseiidae): Is the molecular evidence so evident? *Biol. J. Linn. Soc.* **2010**, *101*, 323–344. [CrossRef]
54. Navia, D.; Domingos, C.A.; Mendonça, R.S.; Ferragut, F.; Rodrigues, M.A.N.; Morais, E.G.F.; Tixier, M.-S.; Gondim, M.G.C. Reproductive compatibility and genetic variability of *Amblyseius largoensis*. *Biol. Control* **2014**, *72*, 17–29. [CrossRef]
55. Meiklejohn, K.A.; Damaso, N.; Robertson, J.M. Assessment of BOLD and GenBank—Their accuracy and reliability for the identification of biological materials. *PLoS ONE* **2019**, *14*, e0217084. [CrossRef] [PubMed]
56. Pentinsaari, M.; Ratnasingham, S.; Miller, S.E.; Hebert, P.D.N. BOLD and GenBank revisited—Do identification errors arise in the lab or in the sequence libraries? *PLoS ONE* **2020**, *15*, e0231814. [CrossRef] [PubMed]
57. Kaminskienė, E.; Radzijevskaja, J.; Griciuvienė, L.; Stanko, M.; Snegiriovaitė, J.; Mardosaitė-Busaitienė, D.; Paulauskas, A. Molecular identification and phylogenetic analysis of Laelapidae mites (Acari: Mesostigmata). *Animals* **2023**, *13*, 2185. [CrossRef] [PubMed]
58. Tixier, M.-S.; Hernandes, F.A.; Guichou, S.; Kreiter, S. The puzzle of DNA sequences of Phytoseiidae in GenBank. *Invertebr. Syst.* **2012**, *25*, 389–406. [CrossRef]


**Disclaimer/Publisher's Note:** The statements, opinions and data contained in all publications are solely those of the individual author(s) and contributor(s) and not of MDPI and/or the editor(s). MDPI and/or the editor(s) disclaim responsibility for any injury to people or property resulting from any ideas, methods, instructions or products referred to in the content.